

Subaru Deep Spectroscopy of a Star-forming Companion Galaxy of BR 1202-0725 at $z = 4.7$ ¹

Youichi Ohyama², Yoshiaki Taniguchi³, & Yasuhiro Shioya³

ABSTRACT

We present deep spatially-resolved optical spectroscopy of the NW companion galaxy of the quasar BR 1202-0725 at $z = 4.7$. Its rest-frame UV spectrum shows star-forming activity in the nuclear region. The Ly α emission profile is symmetric with wavelength while its line width is unusually wide (FWHM $\simeq 1100$ km s⁻¹) for such a high- z star-forming galaxy. Spectrum taken along the Ly α nebula elongation, which is almost along the minor axis of the companion host galaxy, reveals that off-nuclear Ly α nebulae have either flat-topped or multi-peaked profiles along the extension. All these properties can be understood in terms of superwind activity in the companion galaxy. We also find a diffuse continuum component around the companion, which shows similar morphology to that of Ly α nebula, and is most likely due to scattering of the quasar light at dusty halo around the companion. We argue that the superwind could expel dusty material out to the halo region, making a dusty halo for scattering.

Subject headings: quasars: individual (BR 1202-0725) — galaxies: starburst

1. INTRODUCTION

BR 1202–0725 at $z = 4.7$ is one of well-studied quasars at high redshift (e.g., Kennefick, Djorgovski, & Meylan 1996; Ohta et al. 1996; Omont et al. 1996; Hu, McMahon, & Egami 1996; Petitjean et al. 1996; Storrie-Lombardi et al. 1996). A faint companion galaxy is also found to be associated with BR 1202-0725 (Djorgovski 1995). This is located at 2.3'' NW of the quasar (hereafter NW companion) and shows an extended Ly α nebula almost at the same redshift as that of the quasar (Hu et al. 1996; Petitjean et al. 1996; Storrie-Lombardi et al. 1996). Previous optical spectroscopies show that it is a star-forming galaxy with only a narrow Ly α emission (no strong metal emission lines, such as N v, C iv) (e.g., Petitjean et al. 1996; Hu, McMahon, & Egami 1997; Fontana et al. 1998). The redshifted [O II] emission is also detected on the galaxy at near-infrared

²Subaru Telescope, National Astronomical Observatory of Japan, 650 N. A'ohoku Place, Hilo, HI 96720

³Astronomical Institute, Graduate School of Science, Tohoku University, Aramaki, Aoba, Sendai 980-8578, Japan

¹Based on data collected at the Subaru Telescope, which is operated by the National Astronomical Observatory of Japan.

wavelength (Ohta et al. 2000; see also Pahre & Djorgovski 1995 for earlier measurement with only an upper-limit value). Interestingly, redshifted CO emission is detected at another location near the quasar (4'' NW of the quasar), being $\simeq 2''$ away from the NW companion (hereafter, 2nd CO emitter), as well as on the quasar itself (Omont et al. 1996; Carilli et al. 2002; see also Ohta et al. 1996). There are lines of evidence for vigorous star-forming activities at quasar and 2nd CO emitter (e.g., massive content of molecular gas, high excitation temperature of CO lines, optical-FIR SED which is typical of vigorous star-forming galaxies) (e.g., Benford et al. 1996; Omont et al. 1996; Ohta et al. 1996; Ohta et al. 1998; Ohta et al. 2000; Yun et al. 2000; Carilli et al. 2002). Therefore, the ‘‘BR 1202-0725 group’’ seems to contain various kinds of young star-forming objects, and is suitable for investigating star-forming activities in early universe.

Among the three objects in the BR 1202-0725 group, the NW companion would give us an unique opportunity to investigate nature of star formation in a young galaxy because this galaxy appears to be free both from extremely dusty environment and from intense quasar light. Therefore we have made very deep optical spectroscopy of the NW companion with the 8.2m Subaru Telescope, and present our new results in this paper. We assume $\Omega_M = 0.3, \Omega_\Lambda = 0.7, H_0 = 70 \text{ km s}^{-1} \text{ Mpc}^{-1}$ in this paper. 1'' corresponds to 6.7 kpc, in the adopted cosmology.

2. OBSERVATION AND DATA REDUCTION

We used the FOCAS (Kashikawa et al. 2002) attached at Cassegrain focus of the Subaru Telescope (Iye et al. 2004) on Feb. 14 and 15, 2004. A VPH grism (with 600 grooves mm^{-1} and 6500Å central wavelength) and an order-sorting filter Y47 were used to cover a wavelength range from 5950Å to 8400Å. With a combination of a 0.8'' width longslit, this setting provides a spectral resolution of $R = 1700$ (measured with sky lines) near the redshifted Ly α ($\simeq 6930\text{\AA}$). The CCDs were binned onchip to 3×2 (0.3'' \times 0.2'' in space and wavelength directions, respectively). The slit was placed on the companion at two position angles (PAs), at PA= -38.08° (along the quasar and the NW companion: Hu et al. 1996; hereafter, NW-SE slit) on the first night, and at PA= -128.08° (perpendicular to the NW-SE slit; hereafter, NE-SW slit) on the second night (Figure 1). We took eight 30 minute exposures per slit PA (four hours in total). A small nodding of the target along the slit was applied during each exposure. Seeing size was $\simeq 0.5'' - 0.8''$ FWHM during the observations, and was typically 0.6'' FWHM.

Data reduction was made in a standard manner, i.e., bias subtraction, flat fielding, wavelength calibration with Th-Ar arc lines, sky subtraction, and spectral sensitivity calibration with a standard star GD153, were applied. Atmospheric absorption features were corrected with another spectrum of GD153, taken with exactly the same spectroscopy setting as that for the companion. Then, a one-dimensional nuclear spectrum was extracted from the two-dimensional spectra in the following way. First, two nuclear spectra taken at each slit PA were extracted over 0.6'' aperture along the slit around the peak, and then two spectra were coadded. Then, a contamination of the bright quasar light is corrected, by subtracting the scaled quasar spectrum from the observed

spectrum. Here the scale of the quasar spectrum was estimated by measuring the quasar flux at the same distance to the companion but at another side of the quasar ($2.3''$ SE of the quasar) on the spectrum taken along the NW-SE slit. Figure 2 shows the final companion nuclear spectrum as well as the quasar one. Further, we deduced one-dimensional spatial flux distribution of both continuum and Ly α . For each slit PA, two-dimensional spectrum is averaged over the wavelength range of $\lambda > \lambda_{\text{Ly}\alpha}$ and just around $\lambda_{\text{Ly}\alpha}$ to obtain spatial flux distributions of continuum and Ly α , respectively (Figure 3).

3. RESULTS

The nuclear spectrum (Figure 2) is composed of a narrow Ly α emission, almost flat continuum emission at $\lambda > \lambda_{\text{Ly}\alpha}$, and partially absorbed continuum at $\lambda < \lambda_{\text{Ly}\alpha}$. The Ly α emission is detected at $\lambda_{\text{peak}} = 6932\text{\AA}$ (or $z = 4.7026$), and its width is $\simeq 1100 \text{ km s}^{-1}$ FWHM, being consistent with previous results (Petitjean et al. 1996; Fontana et al. 1998). The line profile is almost symmetric along wavelength, except for a narrow absorption line at blue side of the profile ($z = 4.687$, or $\Delta V \equiv V - V_{\text{Ly}\alpha \text{ peak}} \simeq -800 \text{ km s}^{-1}$), and can indeed be reproduced with a Gaussian emission affected by a single absorption line (Figure 2). We point out that, although Petitjean et al. (1996) showed the blue-deficient asymmetric profile of Ly α , such profile seems to be a result of unresolved blue absorption in their lower-quality spectrum.

The nuclear Ly α flux is $f(\text{Ly}\alpha \text{ nuc.}) = 6.5 \times 10^{-17} \text{ erg s}^{-1} \text{ cm}^{-2}$, which is significantly smaller than that of the total one ($f(\text{Ly}\alpha \text{ total}) = 2.7 \times 10^{-16} \text{ erg s}^{-1} \text{ cm}^{-2}$). Note that the total flux, rather than the nuclear one, is consistent with the previously reported values (Hu et al. 1996; Petitjean et al. 1996; Fontana et al. 1998). The continuum spectrum at red side of Ly α ($\lambda > \lambda_{\text{Ly}\alpha}$) shows neither absorption nor emission lines within the observed wavelength range, although rather poor S/N of the continuum spectrum hampered detection of rather weak absorption lines. The continuum flux at 1400\AA , without extinction correction, is $f(\text{continuum}) = 7.3 \times 10^{-32} \text{ erg s}^{-1} \text{ cm}^{-2} \text{ Hz}^{-1}$. At blue side of Ly α ($\lambda < \lambda_{\text{Ly}\alpha}$), the spectrum shows absorbed continuum, which looks very similar to the quasar one showing rich Ly α absorptions and a DLA system (e.g., Storrie-Lombardi et al. 1996).

We found that both the Ly α and the continuum emissions come from extended region out to $3''$ – $4''$ from their peaks along the NE-SW slit, and their flux peaks coincide with each other (Figure 3). This result is slightly different from that of Hu et al. (1996), where they showed that the peak of the Ly α nebula is located about $0.6''$ E from the continuum peak. However, the nebula elongation (NE) appears to be closer to the direction of the peak displacement (E) mentioned by Hu et al. (1996). The Ly α nebula seems to show more centrally concentrated flux distribution comparing with that of the continuum along the slit, especially at the SW side of the companion. The NE nebula is brighter and more extended from the nucleus (distance from the nucleus: $r \simeq 4''$ or $\simeq 27 \text{ kpc}$). At $r = 0.5''$ – $1.5''$ NE, the emission shows flat-topped profile, which is remarkably different from one at nucleus (Figure 4). We found that the profile can be reproduced by a combination

of two Gaussian components (blue and red) at $\Delta V \simeq \pm 400 \text{ km s}^{-1}$, and the line width of each component is $600 - 1200 \text{ km s}^{-1}$ FWHM. At even outer NE regions ($r = 2'' - 3.5''$ NE), the emission shows more complicated shapes, and the profile is probably composed of three velocity components (a near-systemic one at $\Delta V \simeq +200 \text{ km s}^{-1}$, a blue one at $\Delta V \simeq -700 \text{ km s}^{-1}$, and a red one at $\Delta V \simeq +500 \text{ km s}^{-1}$) (see spectrograms in Figure 1, as well as Ly α line profiles in Figure 4). The overall line width, including these three components, is as wide as $\sim 1500 \text{ km s}^{-1}$, and the mean velocity is close to the systemic velocity ($|\Delta V| \lesssim 200 \text{ km s}^{-1}$). At another side of the companion, the SW nebula, is fainter and more compact in space ($\simeq 3''$ or $\simeq 20 \text{ kpc}$). At $r = 0.5'' - 2.5''$ SW, the profile looks similar to that at outer NE nebula, although the profile looks composed of two brighter components at blue ($\Delta V \simeq -400 \text{ km s}^{-1}$) and near-systemic velocity ($\Delta V \simeq 0 \text{ km s}^{-1}$) as well as a possible fainter component at red ($\Delta V \sim +500 \text{ km s}^{-1}$) which is barely visible on a smoothed spectrogram.

Compared with the NE-SW extension, the extension along the NW-SE slit is much less prominent, although Ly α nebula is slightly more extended than that for the continuum. There is an extension toward NW (toward 2nd CO emitter) out to $r \simeq 2''$ ($\sim 14 \text{ kpc}$). The profile there looks more complicated than that the NE nebula, and is probably composed of two narrow components with overall velocity extent of as wide as 1000 km s^{-1} at its mean velocity of $\Delta V \sim +500 \text{ km s}^{-1}$. At another side of the quasar toward SE, fainter and narrow ($\sim 500 \text{ km s}^{-1}$ FWHM) extension is detected ($r \simeq 1''$, or $\simeq 7 \text{ kpc}$). There is no major velocity structure along the extension ($|\Delta V| \lesssim 200 \text{ km s}^{-1}$), although details of its kinematical properties are not well known due to contamination of brighter quasar light. These properties (extent and velocity structure) of the nebula along the NW-SE slit are consistent with the report of Fontana et al. (1998). We also note that there is a nebula extension even at SE of the quasar ($r \sim 4''$) at $\Delta V \sim -500 \text{ km s}^{-1}$ (see a spectrogram in Figure 1). Since we do not have any detailed information for it, no discussions will be made on it.

4. DISCUSSION

4.1. Star-Formation Activity of the NW Companion

The NW companion shows the following distinct characteristics: (1) It has a narrow [FWHM(NW companion) \ll FWHM(quasar)] Ly α emission, whose redshift is very close to that of quasar. (2) Its continuum spectrum shows a step in flux between blue and red sides of Ly α . (3) It has no strong metal emission lines, such as N v and C iv, being suggestive of AGN activity. All these indicate that the companion is a star-forming galaxy which is physically associated with BR 1202-0725 quasar. We estimate the star-forming rate (SFR) to be $\simeq 13 M_{\odot} \text{ yr}^{-1}$ based on the relation of Kennicutt (1998) and the estimated continuum luminosity at 1500\AA from our measurement at 1400\AA . Note that the Ly α luminosity seems not useful for estimating SFR, because Ly α emission from the extended nebula, which is likely to be excited by shock, may contribute to the nuclear Ly α flux (see later sections for details).

Properties of the companion host galaxy is examined by using a stellar continuum color of I and K . We do not use R data, because it includes a strong $\text{Ly}\alpha$ emission and bluer-than- $\text{Ly}\alpha$ continuum, both of which are difficult to be modeled. We adopt $I = 24.1 \pm 0.2$ and $K = 23.4 \pm 0.4$ from Fontana et al. (1996) and Hu et al. (1996), and a contribution of redshifted $[\text{O II}]\lambda 3727$ in K is corrected based on $[\text{O II}]$ equivalentwidth measured by Ohta et al. (2000). Continuum emission from the ionized gas is neglected here, because such continuum emission is generally much fainter than that of stellar continuum in starburst galaxies. We adopt a synthetic stellar spectrum model “starburst 99” (Leitherer et al. 1999) to match the observed color. We adopt instantaneous burst models (IMF slope $\alpha = 2.35$, $M_{\text{up}} = 100 M_{\odot}$, $M_{\text{low}} = 1 M_{\odot}$, $Z = 1/5Z_{\odot}$ or $Z = 1/20Z_{\odot}$) with various ages (5-50 Myr). Here we fix IMF parameters, and ignore the reddening effect for simplicity. By comparing models and the observed color, we found that models of lower metallicity ($\simeq 1/20Z_{\odot}$) and younger age (10 Myr) better represent the observations (Figure 5). It seems important to note that the observed blue UV color can only be reproduced if almost no reddening is applied on the young stellar population with bluest color.

4.2. Nature of the Extended $\text{Ly}\alpha$ Nebula

4.2.1. Kinematic Properties of the Nebula

Although the NW companion shows characteristic properties for star-forming galaxies, it also shows unusual properties for such a high- z star-forming galaxy: (1) At the nucleus, $\text{Ly}\alpha$ emission profile is wide ($\simeq 1100 \text{ km s}^{-1}$ FWHM) and almost symmetric in wavelength, being different from narrower ($200 - 400 \text{ km s}^{-1}$ FWHM) and blue-deficient asymmetric profiles which are typical for such a high- z star-forming galaxy (e.g., Dawson et al. 2002; Ajiki et al. 2002; Kodaira et al. 2003; Rhoads et al. 2003; see for a review Taniguchi et al. 2003 and references therein). (2) At the off-nucleus, the companion show an extended $\text{Ly}\alpha$ nebula with a complicated velocity structure, whose overall velocity width is as wide as $\sim 1500 \text{ km s}^{-1}$ ². If we assume that an extended nebula with such a violent kinematical status surrounds the companion, we could expect that the high velocity component ($|\Delta V| > 300 \text{ km s}^{-1}$) on the nucleus arises from the nebula along our line-of-sight toward the companion nucleus. If this is the case, the NW companion is likely composed of a usual star-forming galaxy and the surrounding extended nebula with violent kinematical status.

Here a question arises as what is the origin of the extended nebula. There seems several possibilities: (1) scattering of the quasar light by circumgalactic gas, (2) photoionization of circum-

²Since $\text{Ly}\alpha$ is a resonance line, the observed $\text{Ly}\alpha$ profile might be strongly affected by the neutral gas around the companion (see, e.g., Mas-Hesse et al. 2003). However, since nuclear $\text{Ly}\alpha$ profile does not show a blue-deficient profile, and the overall velocity extent of the $\text{Ly}\alpha$ profile (e.g., blue/red tip velocity of the profile) is almost symmetric around the peak of the nuclear $\text{Ly}\alpha$ profile at off-nuclear regions (except for NW and SW tip of the nebula), we think that effect of the neutral gas for the observed $\text{Ly}\alpha$ profile could be rather small. Therefore, we assume in the following that the observed $\text{Ly}\alpha$ profile is determined by kinematical and/or excitation structures of the ionized gas.

galactic gas by the quasar UV light, (3) spatially extended star-formation of the companion, (4) cooling radiation from protogalaxies within dark matter halos (e.g., Haiman, Spaans, & Quataert 2000), and (5) galaxy-scale shock heating. First possibility can be rejected due to different spectrum shape between the nebula and the quasar. Second possibility seems less likely since no strong emission lines suggestive of AGN excitation, such as N v, are detected. Third and fourth possibilities seem also less likely since they could not explain straightforwardly the observed kinematical structure of the nebula, such as wide line width and flat-topped/multi-peaked profiles. Also, the third possibility is less likely because the host galaxy elongates along NW-SE directions (Hu et al. 1996), being perpendicular to the direction of the nebula elongation. Therefore, the last possibility seems most feasible, since shock could be excited within the nebula showing the observed violent kinematical structure, and it can emit intense Ly α emission (e.g., Shull & McKee 1979), if we assume that some kind of mechanism works to produce a violent internal motion of the nebula.

We showed that the Ly α profile in the NE nebula can be composed of two (blue and red) or three (blue, near-systemic, and red) components at inner and outer parts of the nebula, respectively (see section 3). We note that the inner nebula, which appears to show only two components, could be composed of three components, and the fainter and narrower near-systemic one was missed due to nearby brighter and wider components. The SW nebula also seems to have two (blue and near-systemic) components, and a possibly fainter red component. One may think that these nebulae show similar kinematical properties, and might form a single, large, elongated nebula at both sides of the companion along its minor axis. An idea to explain a pair of blue and red components at a same position within the nebula is to introduce an expanding or contracting shell of ionized gas, in which each component comes from either front or back side of the shell. A near-systemic component may be attributed to other component, e.g., a dusty halo without violent motion or scattering the companion nuclear light, although we can not discriminate these ideas.

4.2.2. *The Superwind Model*

Because of the vigorous star-formation activity of the NW companion, it seems natural to expect a superwind activity associated with the companion. The superwind blows at later phase of the starburst evolution when the large number of OB stars die as supernovae (SNe) and release huge kinetic energy into circumnuclear region, and a circumnuclear bubble of shock-heated hot ionized gas expands eventually out to halo area (see, e.g., Heckman, Armus, & Miley 1990 for details). During the course of expansion, the bubble interacts with dense gas within the galactic disk, and it preferentially elongates along the disk polar direction where the density is smallest. The nebula emits UV-optical emission lines (including Ly α) by shock heating occurring around the hot gas bubble where it interacts with ambient cold matter. Therefore, the superwind nebula often forms an expanding shell or bubble, being capable of producing a pair of blue- and red-shifted nebula emissions. Since the companion shows a “linear” or highly elongated disk-like structure in continuum along NW-SE direction (Hu et al. 1996), the superwind nebula, if any, would show

elongation along NE-SW direction, being consistent with the observation. Superwind nebula can extend as large as a few kpc – several tens kpc, and the wind velocity can be as fast as a few – several hundreds km s^{-1} (e.g., Heckman et al. 1990). Therefore, the superwind model can explain velocity structure and morphology of the nebula in a qualitative way. An axis of the superwind outflow is likely to be close to the sky plane, as expected from the highly elongated appearance of the host galaxy, and this could help to explain weak velocity shear along the nebula extension.

According to the galactic wind theory (e.g., Arimoto & Yoshii 1987), the star formation ceases when the galactic wind blows out. Therefore, the youngest stellar population, which has born when the wind just started to blow out, will contribute most to the observed UV light due to largest UV luminosity/mass ratio, if SFR is almost constant while star-bursting. Since the blue UV color indicates an age of the stellar population as ~ 10 Myr, the wind age (or timescale of the wind propagation) is likely to be ~ 10 Myr. If this is the case, the superwind nebula could extend out to $\simeq 4 \text{ kpc}/f$ (or $\simeq 0.6''/f$), assuming a constant wind speed of $V_{\text{exp}} = (1/2 \text{ of velocity separation of blue- and red-Gaussian components at off-nuclear region})/f \simeq 400 \text{ km s}^{-1}/f$, where f is a geometrical conversion factor for calculating transverse velocity from the line-of-sight velocity. This estimate is consistent with the observed typical nebula size ($\simeq 3''$) if f is $\sim 1/5$. Therefore, all information (stellar color, line width, and nebula size) can be understood in a context of the superwind model, although all the estimates are based on a simple and/or order-of-magnitude calculation.

4.3. Origin of Diffuse Continuum Component around the Companion

We showed that the continuum emission extends spatially along the NE-SW slit over $\pm 3''$ from the companion nucleus. Since the $\text{Ly}\alpha$ nebula shows more concentrated flux distribution around the nucleus, this component should show a continuum-dominated spectrum at $\lambda > \lambda_{\text{Ly}\alpha}$, especially at SW side of the companion (Figure 3). Therefore, neither of scattering of the companion light, photoionization either by the quasar nor the companion are likely as an origin of the component, since all these models would create a $\text{Ly}\alpha$ -dominated spectrum. Therefore, the most likely origin of the component is a scattering of the quasar light at circumgalactic matter.

The HST image also reveals a diffuse continuum structure around the companion (Figure 1). This component seems to show similar morphology to that of the $\text{Ly}\alpha$ nebula, i.e., the elongation is found along NE-SW direction but not toward NW (information toward SE is lost due to bright quasar light). Therefore, the medium for the quasar light scattering is likely to be associated with the NW companion. Here, a question arises as how such a component is created around the companion. There are several possibilities: (1) tidal structures around the companion made during merging process of the companion, quasar, and the 2nd CO emitter, (2) pre-galactic clumps remaining around the companion, (3) dusty ejecta from the companion, and (4) genuine dusty halo of the companion. Although we could not discriminate these possibilities, the third possibility seems more likely, because neutral matter could be transferred from dusty nuclear region out to

halo as well as the ionized gas within a context of superwind model (Heckman et al. 2000 and references therein). If this is the case, we can explain similar morphological properties between Ly α nebula and the continuum structure. Because there are plenty of molecular gas (and hence dusts) within the BR 1202-0725 group (at quasar and 2nd CO emitter), it seems natural to consider that the star formation occurred in a dusty environment also in the companion. If we assume that the dusty circumnuclear material has been expelled by the superwind outflow, we might explain a current weak-reddening nuclear environment of the companion.

REFERENCES

- Ajiki, M., et al. 2002, *ApJ*, 576, L25
- Arimoto, N., & Yoshii, Y. 1987, *A&A*, 173, 23
- Benford, D. J., Cox, P., Omont, A., Phillips, T. G., & McMahon, R. G. 1999, *ApJ*, 518, L65
- Carilli, C. L., Kohno, K., Kawabe, R., Ohta, K., Henkel, C., Menten, K. M., Yun, M. S., Petric, A., & Tutui, Y. 2002, *AJ*, 123, 1838
- Dawson, S., Spinrad, H., Stern, D., Dey, A., van Breugel, W., de Vries, W., & Reuland, M. 2002, *ApJ*, 570, 92
- Djorgovski, S. G. 1995, in *Science with the VLT*, ed. J. R. Walsh & I. J. Danziger (Berlin: Springer), 351
- Hu, E. M., McMahon, R. G., & Egami, E. 1996, *ApJ*, 459, L53
- Hu, E. M., McMahon, R. G., & Egami, E. 1997, in *The Hubble Space Telescope and the High Redshift Universe*, ed. N. R. Tanvir, A. Aragon-Salamanca, & J. V. Wall (Singapore: World Scientific), 91
- Fontana, A., D’Odorico, S., Giallongo, E., Cristiani, S., Monnet, G., & Petitjean, P. 1998, *AJ*, 115, 1225
- Guilloteau, S., Omont, A., Cox, P., McMahon, R. G., & Petitjean, P. 1999, *A&A*, 349, 363
- Iye, M., et al. 2004, *PASJ*, 56, 381
- Haiman, Z., Spaans, M., & Quataert, E. 2000, *ApJ*, 537, L5
- Heckman, T. M., Armus, L., & Miley, G. K. 1990, *ApJS*, 74, 833
- Heckman, T. M., Lehnert, M. D., Strickland, D. K., & Lee, A. 2000, *ApJS*, 129, 493
- Kashikawa, N., et al. 2002, *PASJ*, 54, 819
- Kennefick, J. D., Djorgovski, S. G., & Meylan, G. 1996, *AJ*, 111, 1816
- Kennicutt, R. C., Jr. 1998, *ARA&A*, 36, 189
- Kodaira, K., et al. 2003, *PASJ*, 55, L17
- Leitherer, C., Schaerer, D., Goldader, J. D., Delgado, R. M., González, R., Robert, C., Kune, D. F., de Mello, D. F., Devost, D., & Heckman, T. M. 1999, *ApJS*, 123, 3
- Mas-Hesse, J. M., Kunth, D., Tenorio-Tagle, G., Leitherer, C., Terlevich, R. J., & Terlevich, E. 2003, *ApJ*, 598, 858
- Ohta, K., Yamada, T., Nakanishi, K., Kohno, K., Akiyama, M., & Kawabe, R. 1996, *Nature*, 382, 426
- Ohta, K., Nakanishi, K., Akiyama, M., Yamada, T., Kohno, K., Kawabe, R., Kuno, N., & Nakai, N. 1998, *PASJ*, 50, 303

- Ohta, K., Matsumoto, T., Goto, M., Motohara, K., Taguchi, T., Hata, R., Yoshida, M., Iye, M., Simpson, C., & Takta, T. 2000, PASJ, 52, 557
- Omont, A., Petitjean, P., Guilloteau, S., McMahon, R. G., Solomon, P. M., & Pécontal, E. 1996, Nature, 382, 428
- Pahre, M. A., & Djorgovski, S. G. 1995, ApJ, 449, L1
- Petitjean, P., Pécontal, E., Valls-Gabaud, D., & Charlot, S. 1996, Nature, 380, 411
- Rhoads, J. E., Dey, A., Malhotra, S., Stern, D., Spinrad, H., Jannuzi, B. T., Dawson, S., Brown, M. J. I., & Landes, E. 2003, AJ, 125, 1006
- Shull, J. M., & McKee, C. F. 1979, ApJ, 227, 131
- Storrie-Lombardi, L. J., McMahon, R. G., Irwin, M. J., & Hazzard, C. 1996, ApJ, 468, 121
- Taniguchi, Y., Shioya, Y., Fujita, S. S., Nagao, T., Murayama, T., & Ajiki, M. 2003, JKAS, 36, 123 (astro-ph/0306409); Erratum, JKAS, 36, 283
- Yun, M. S., Carilli, C. L., Kawabe, R., Tutsui, Y., Kohno, K., & Ohta, K. 2000, ApJ, 528, 171

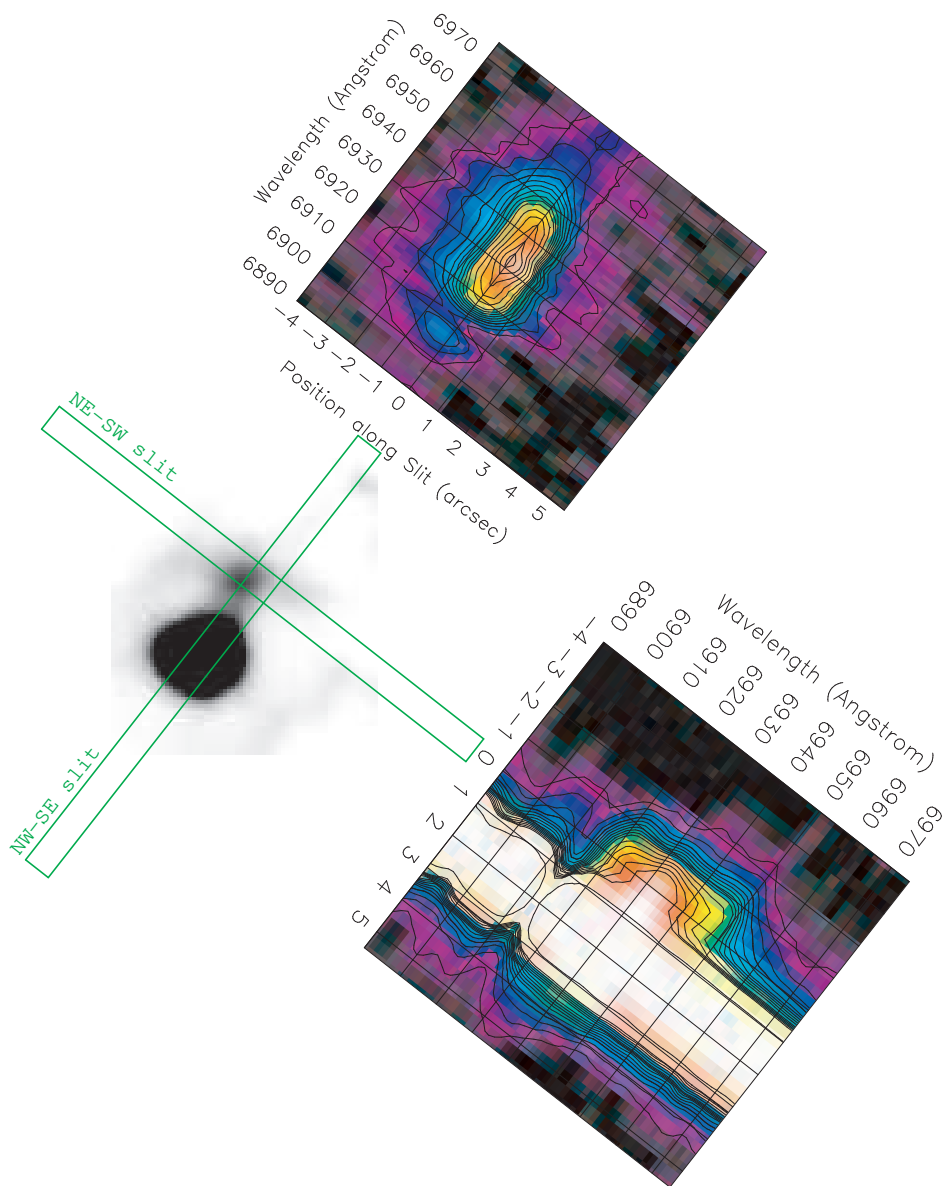
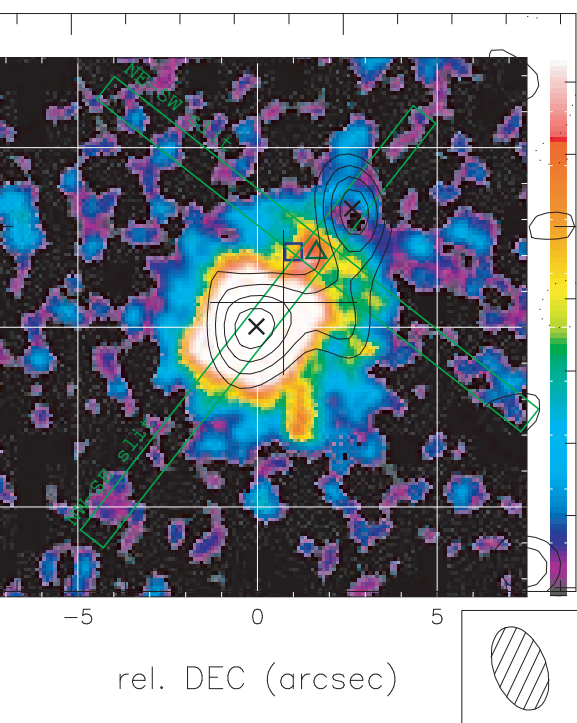
Fig. 1.— Slit positions are shown on a HST F814W (left) and a narrow-band Ly α (middle) images of Hu et al. (1996). The HST F814W image was made by us from archival data. A radio-continuum image at 1.35 mm (Guilloteau et al. 1999) is superimposed on the F814W image. All these images are shown at a same scale. Positions of the NW companion seen in the F814W and the Ly α images are marked with triangle and square on the F814W image, respectively. Ly α spectrograms are shown along each slit position. The spectrograms are smoothed with a 3×3 boxcar kernel to enhance the velocity structure at fainter and outer nebulae.

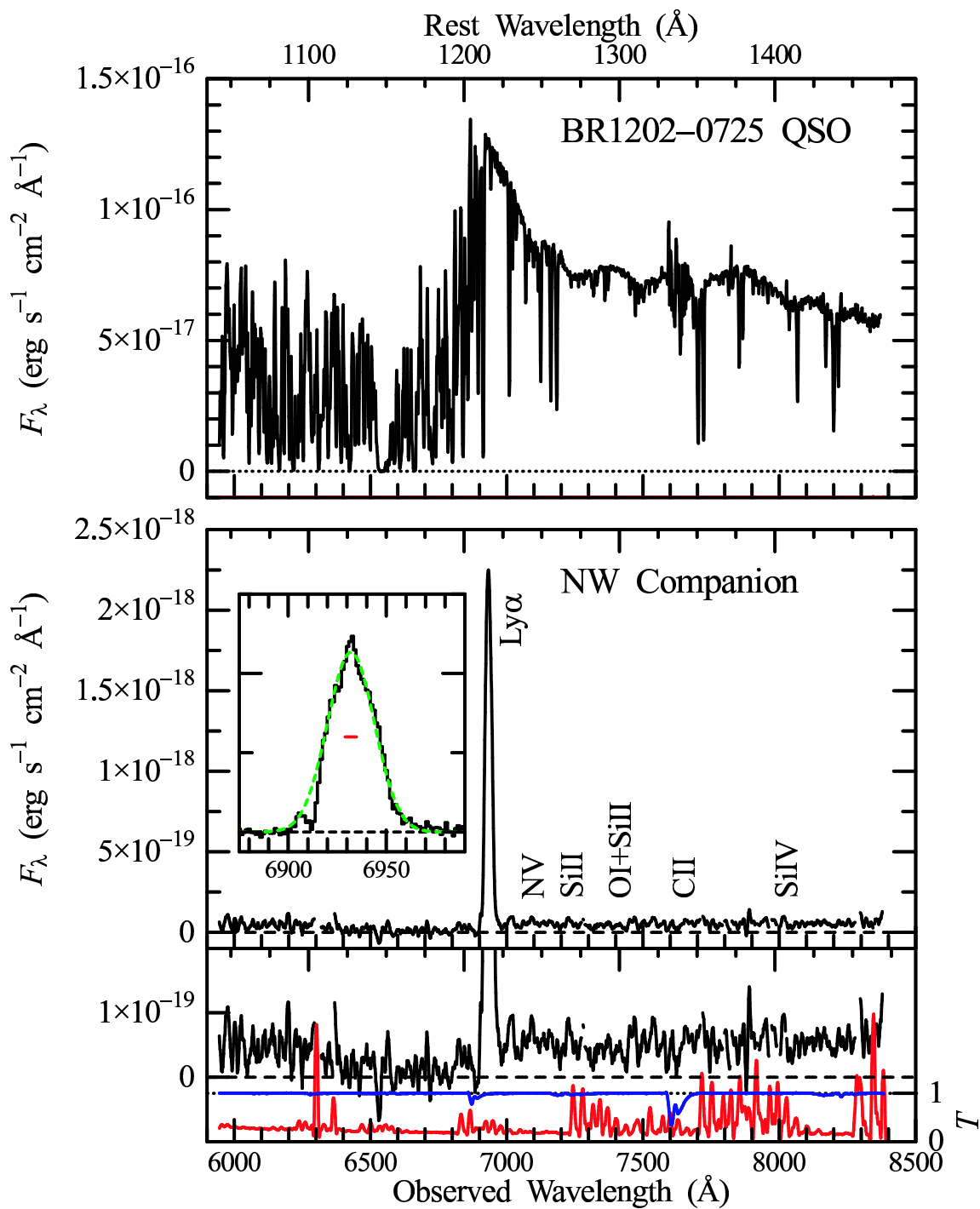
Fig. 2.— Observed spectra of quasar (top) and the NW companion (bottom). The bottom panel contains sub-panels for close-ups of the Ly α profile and the continuum spectrum, as well as the scaled sky spectrum (in red) and the atmospheric transmission curve (in blue). In a sub-panel of the Ly α profile, a fitted Gaussian emission profile is overlaid on the observed profile (in green), as well as a horizontal tick mark showing the instrumental spectral resolution (in red). Expected positions for emission/absorption lines are also indicated along the spectrum.

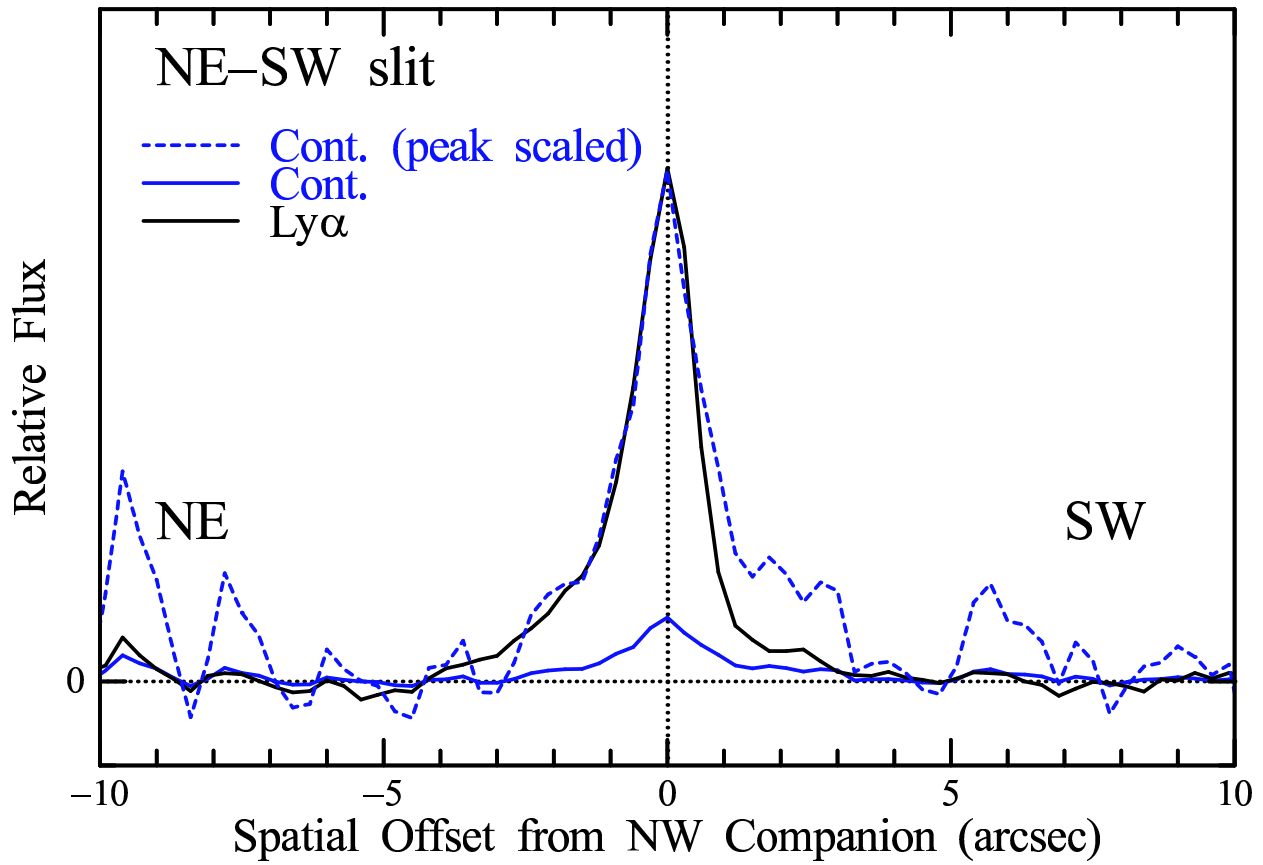
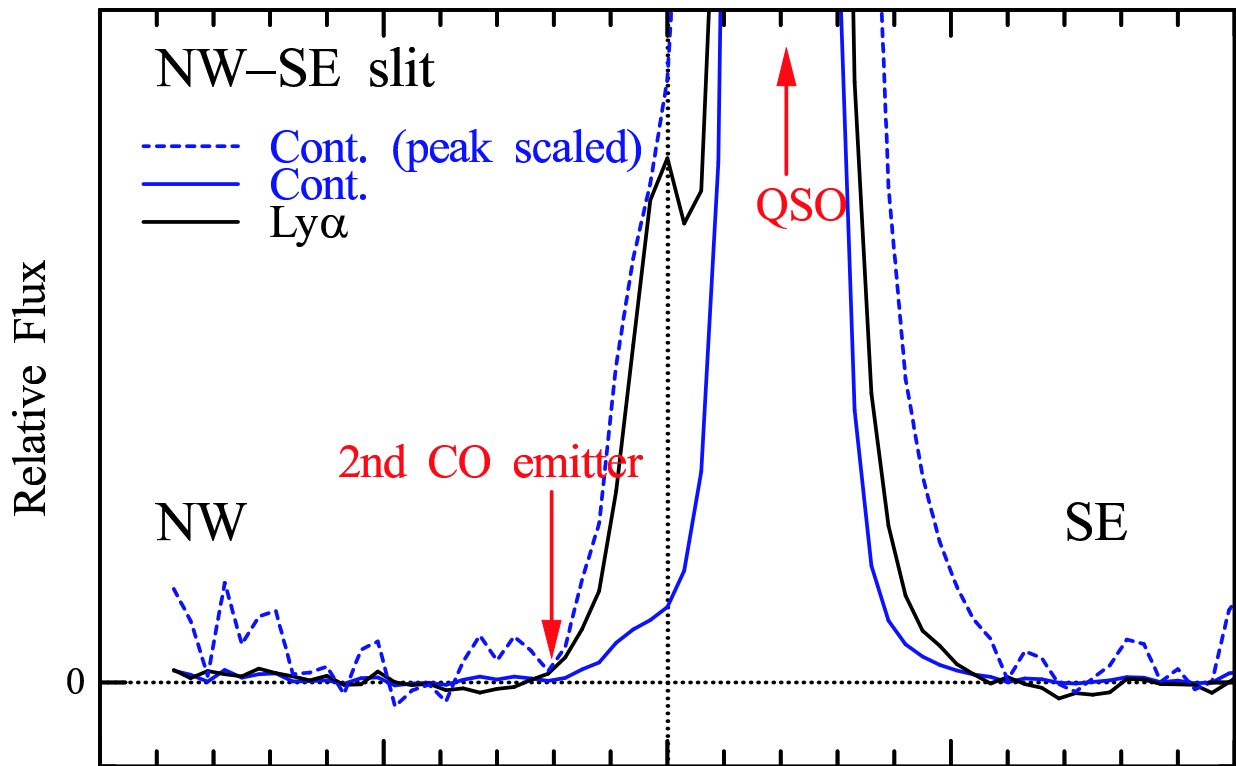
Fig. 3.— Averaged spatial flux distributions are shown along NW-SE slit (upper) and NE-SW slit (below) for Ly α (in black) and continuum (in blue), separately. In each plot, dashed blue lines show the continuum flux distribution scaled to match that of the Ly α near their peaks, which make it easier to compare the spatial flux distributions of Ly α and continuum. Relative flux scales for both panels are same. Positions of accompanying objects (2nd CO emitter and the quasar) are marked in the upper panel.

Fig. 4.— Ly α profiles are shown along each slit at $0.6''$ step. Results of the profile decomposition at $0.6''$ NE nebula are overlaid on the observed spectrum, with blue- and red-shifted Gaussian components (in blue and red, respectively) and their sum (in green), as well as the fitting residual (in pink) and the zero flux level (in yellow).

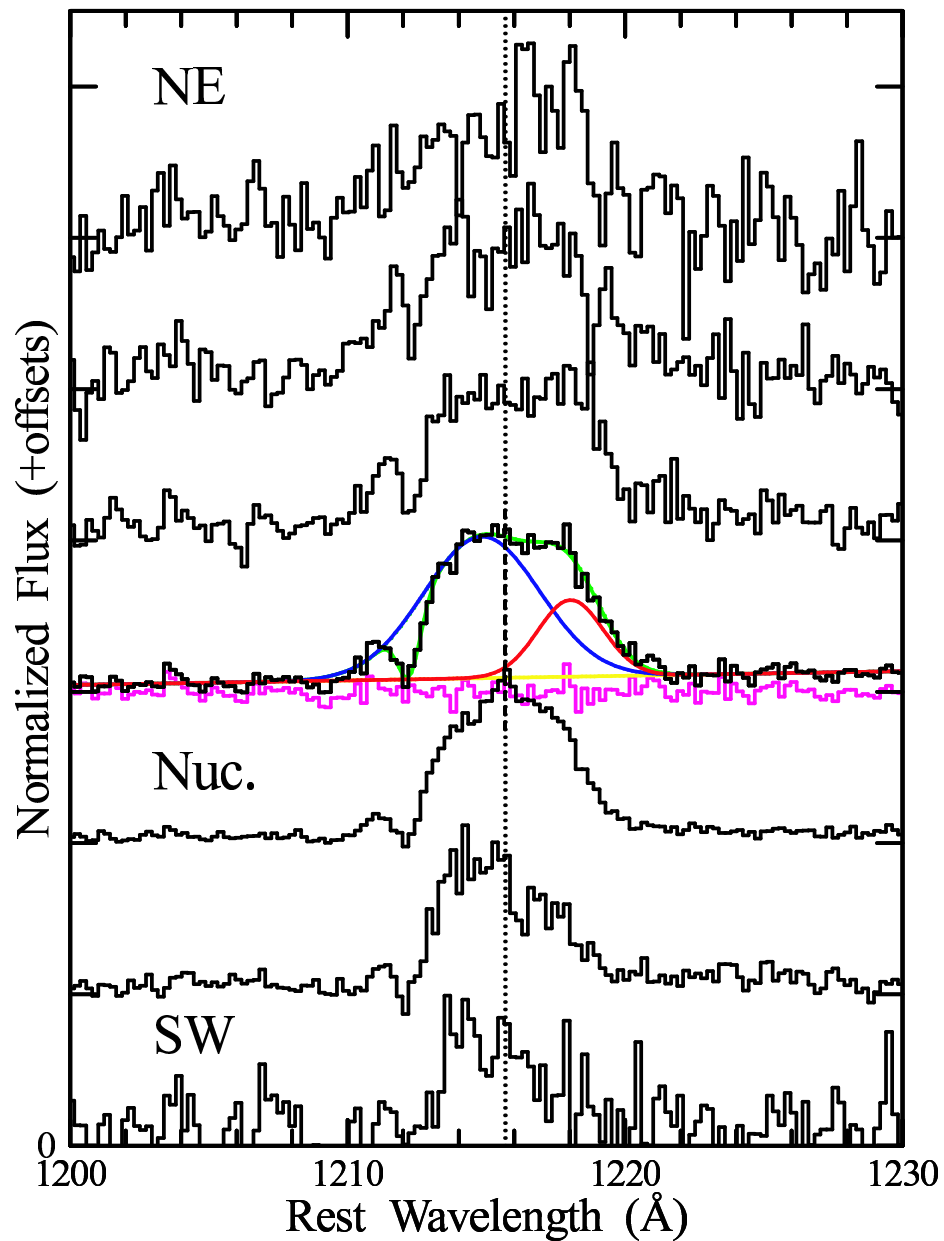
Fig. 5.— Comparison of the observed continuum luminosities and synthetic models are made. Observed I (in black) and K (in pink) luminosities are shown as well as [O II] emission-corrected stellar K luminosity (in black). Synthetic stellar continua of the instantaneous burst models at various ages (5 – 50 Myr) are shown for the cases of metallicities of $Z = 1/5Z_{\odot}$ (upper) and $Z = 1/20Z_{\odot}$ (lower). All model continua are normalized at I band.







Along NE–SW Slit



Along NW–SE Slit

